European Journal of Medicinal Chemistry 84 (2014) 687–697

Contents lists available at ScienceDirect

European Journal of Medicinal Chemistry

journal homepage: http://www.elsevier.com/locate/ejmech

Original article

2-(4-Chlorobenzyl)-6-arylimidazo[2,1-*b*][1,3,4]thiadiazoles: Synthesis, cytotoxic activity and mechanism of action

Sujeet Kumar [a, 1], Mahesh Hegde [b, 1], Vidya Gopalakrishnan [b], Vinaya Kumar Renuka [a], Sureshbabu A. Ramareddy [a], Erik De Clercq [d], Dominique Schols [d], Anil Kumar Gudibabande Narasimhamurthy [c], Sathees C. Raghavan [b], Subhas S. Karki [a, *]

[a] Department of Pharmaceutical Chemistry, KLE University's College of Pharmacy, Bangalore 560010, India
[b] Department of Biochemistry, Indian Institute of Science, Bangalore 560012, India
[c] Dept. of Physics, M. S. Ramaiah Institute of Technology, Bangalore 560054, India
[d] Rega Institute for Medical Research, KU Leuven, B-3000 Leuven, Belgium

ARTICLE INFO

Article history:
Received 11 June 2013
Received in revised form
15 July 2014
Accepted 16 July 2014
Available online 17 July 2014

Keywords:
Anti-cancer drugs
Cancer therapeutics
Cytotoxicity
Apoptosis
Cell death

ABSTRACT

The cytotoxic activity of a new series of 2-(4′-chlorobenzyl)-5,6-disubstituted imidazo[2,1-*b*][1,3,4] thiadiazoles against different human and murine cancer cell lines is reported. Among the tested compounds, two derivatives namely 2-(4-chlorobenzyl)-6-(2-oxo-2H-chromen-3-yl)imidazo[2,1-*b*][1,3,4] thiadiazole-5-carbaldehyde **4i** and 2-(4-chlorobenzyl)-6-(2-oxo-2H-chromen-3-yl)imidazo[2,1-*b*][1,3,4] thiadiazol-5-yl thiocyanate **5i** emerged as the most potent against all the cell lines. To investigate the mechanism of action, we selected compounds **4i** for cell cycle study, analysis of mitochondrial membrane potential and Annexin V-FITC flow cytometric analysis and DNA fragmentation assay. Results showed that **4i** induced cytotoxicity by inducing apoptosis without arresting the cell cycle.

1. Introduction

Cancer is a class of diseases in which cells, or a group of cells display uncontrolled growth, invasion, and sometimes metastasis. It affects people at all ages with the risk of most types increasing with age. Earlier we reported on the antitumor activity of 2-aralkyl-5-substituted-6-(4-fluorophenyl)imidazo[2,1-*b*][1,3,4]thiadiazoles [1] which were mainly synthesized according to Scheme 1. Thus, the 2-amino-5-(4-chlorobenzyl)-1,3,4-thiadiazole **1** was treated with 4-fluorophenacyl bromide to obtain compound **2a** (R = C_6H_4-4-F) [1]. This compound served as a precursor of the bromo-, formyl- and thiocyanate derivatives (**3a**), (**4a**) and (**5a**) (R = C_6H_4-4-F), respectively [1]. The promising results obtained in the cytotoxicity assays prompted us to prepare second-generation derivatives where the 4-fluorophenyl group was replaced by other substituted phenyl rings or by a coumarin-3-yl group [2–4]. It is known that the substitution on C-5 is important for cytotoxic activity. As will be seen in the Results and discussion section, this approach yielded new compounds with improved activity against several tumor cell lines, which was superior to standard antitumorals such as melphalan or parental compound Levamisole.

2. Chemistry

In order to determine structure–activity (SAR) relationships, 36 compounds were prepared according to the strategy outlined in Scheme 1. Different 2-bromoketones were used in the first step, to afford compounds **2a**–**i** (Table 1). The bromination step was carried out with bromine in glacial acetic acid, yielding compounds **3a**–**i**, while the formylation used standard Vilsmeier conditions to give compounds **4a**–**i**. The thiocyanation was performed by treatment with bromine and potassium thiocyanate, affording products **5a**–**i** (Table 1).

3. Results and discussion

3.1. Chemistry

All the synthesized compounds showed absorption bands ranging from 3185 to 3004 cm^{-1} for C–H aromatic stretching and

* Corresponding author.
E-mail address: subhasskarki@gmail.com (S.S. Karki).
[1] Equal first authors.

http://dx.doi.org/10.1016/j.ejmech.2014.07.054
0223-5234/

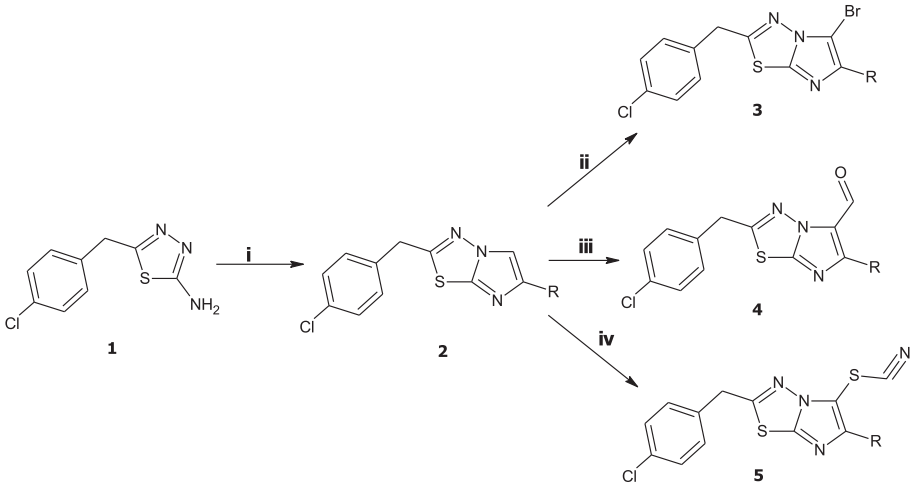

Reagents & conditions: i) $RCOCH_2Br$, Na_2CO_3, alcohol, reflux; ii) Br_2, CH_3COOH; iii) DMF, $POCl_3$, 80-90°C, Na_2CO_3; iv) KSCN, Br_2, CH_3COOH.

Scheme 1. Synthesis of 2,5,6-substituted imidazo[2,1-*b*][1,3,4]thiadiazoles.

2980–2824 cm^{-1} for C–H aliphatic stretching. Compounds **4a**–**i** showed vibration bands between 1672 and 1653 cm^{-1} for C=O stretching. Compounds **5a** to **5i** showed vibration bands at 2163–2157 cm^{-1} for SCN in their respective IR spectra.

In ^1H NMR, the presence of singlet between δ 8.64 and 7.88 ppm for the imidazole proton (C_5–H) confirmed the cyclization of 2-amino-5-(4-chlorobenzyl)-1,3,4-thiadiazole **1** with respective phenacyl bromide. All the electrophilic substitution reactions carried out on imidazo[2,1-*b*][1,3,4]thiadiazole derivatives **2a**–**i**, afforded the expected 5-substituted derivatives (**3a**–**i**, **4a**–**i**, **5a**–**i**). All these 5-substituted derivatives showed the absence of C_5–H in their respective spectra and confirmed the substitution at C-5 position. Derivatives **4a**–**i** showed a singlet between δ 10.08 to 9.94 ppm for the CHO proton. All the compounds showed prominent signals for aromatic protons around δ 8.91–6.92 ppm. Bridge headed methylene proton at C_2 appeared between δ 4.60 to 4.26 ppm for all derivatives. The compounds **2d**, **3d**, **4d**, and **5d** showed OCH_3 proton between δ 3.84–3.78 ppm. Compounds **2e**, **3e**, **4e** and **5e** showed a methyl proton between δ 2.37–2.32 ppm as singlet. The structures of all the compounds were finally ascertained by mass spectra. In the case of a representative compound (**3b**), the structure was also determined by X-Ray analysis, as commented upon in the Supporting information section.

3.2. Bioevaluations

The cytotoxic activities of the 36 compounds were evaluated against human HeLa cervical carcinoma, CEM T-lymphocytes and murine L1210 leukemia cells, and the most potent compounds were studied for their cytotoxicity against REH and K562 cells. The mode of cytotoxic action was also studied using REH and K562 cells, as described below.

3.2.1. Cytotoxicity in human & murine tumor cell lines

The evaluation of the compounds in Scheme 1 towards human cervix carcinoma HeLa and T-lymphocyte CEM cells as well as murine leukemia L1210 cells was undertaken in order to determine whether the compounds were cytotoxic to human transformed cells. The data are presented in Table 2 in comparison with melphalan and levamisole.

There was not much improvement in cytotoxic activity of compounds **2a**–**i** with respect to standard. When a bromine group was introduced at the 5th position of the imidazo[2,1-*b*][1,3,4] thiadiazole moiety resulting in the formation of 5-bromo derivatives (**3a**–**i**), the IC_{50} value of the coumarin analog (compound **3i**, IC_{50} 3.7–5.2 μM) towards all cell lines was, at average, two times less potent, than the reference drug melphalan (IC_{50} 1.4–2.1).

However, when the –CHO group was introduced at the C-5 position of the imidazo[2,1-*b*][1,3,4]thiadiazole moiety, which resulted in the formation of the 5-formyl derivatives (**4a**–**i**), there was much improvement in cytotoxicity towards all three-cell lines by compounds **4c**, **4d** and **4i** (IC_{50} 0.7–6.0 μM). Compound **4i** was three times more cytostatic against L1210, CEM and HeLa tumor cells than melphalan.

In separate experiments, when the –SCN group was introduced at the C-5 position of the imidazo[2,1-*b*][1,3,4]thiadiazole moiety, which resulted in the formation of 5-thiocyanate derivatives (**5a**–**i**), the cytotoxicity of compound **5i** (IC_{50} 1.0–1.4 μM) was two times more potent against all cell lines tested.

The structure–activity relationship has been studied at the C-5 and C-6 position in the skeleton of imidazo[2,1-*b*][1,3,4]thiadiazole. Substitution of bromine at C-5 position did not produce any improvement in cytotoxicity activity, except for compound **3i** (IC_{50} 3.7–5.2 μM) with the coumarin moiety at the C-6 position. Introduction of a formyl group at the C-5 position by Vilsmeier reaction resulted in improvement of cytotoxic activity (see compounds **4c** IC_{50} 4.0–4.6 μM, **4d** IC_{50} 3.8–6.0 μM and **4i** IC_{50} 0.7–0.9 μM). Replacement of the phenyl group at the C-6 by a coumarin-3-yl group gave compound **4i** with an IC_{50} of 0.89 μM, 0.75 μM and 0.90 μM for L1210, CEM & HeLa, respectively. In the next step of modification, –SCN group was introduced at the C-5 position and produced an improvement in cytotoxic activity (compounds **5a**, **5d**, **5g** & **5i**) in the range of 1.0 μM–24 μM for all three cell lines.

The compounds **4i** and **5i** exhibited highest levels of cytotoxicity, based on above studies and were tested further in two leukemia cell lines to evaluate their mechanism of action (Table 3).

3.2.2. *4i* and *5i* induce cytotoxicity in leukemic cells

In the present study we have used two leukemic cell lines, REH and K562 to evaluate the cytotoxic effects of **4i** and **5i** (Fig. 1).

Table 1
Structure and molecular weight of imidazo[2,1-*b*][1,3,4]thiadiazoles (**2a**–**i**, **3a**–**i**, **4a**–**i**, and **5a**–**i**).

Structure	R	Code	Mol formula	Mol wt	MP (°C)
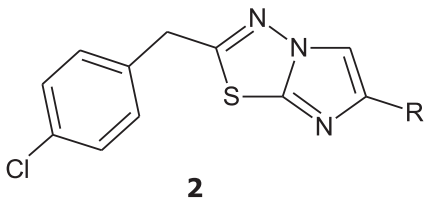 **2**	4-F-ph	a	$C_{17}H_{11}ClFN_3S$	343.81	167–170
	4-Cl-ph	b	$C_{17}H_{11}Cl_2N_3S$	360.26	178–179
	4-Br-ph	c	$C_{17}H_{11}BrClN_3S$	404.71	164–165
	4-OCH_3-ph	d	$C_{18}H_{14}ClN_3OS$	355.84	174–176
	4-CH_3-ph	e	$C_{18}H_{14}ClN_3S$	339.84	178–181
	2,4-di-Cl-ph	f	$C_{17}H_{10}Cl_3N_3S$	394.71	144–147
	Ph	g	$C_{17}H_{12}ClN_3S$	325.82	193–195
	4-NO_2-ph	h	$C_{17}H_{11}ClN_4O_2S$	370.81	195–198
	Coumarin-3-yl	i	$C_{20}H_{12}ClN_3O_2S$	393.85	202–205
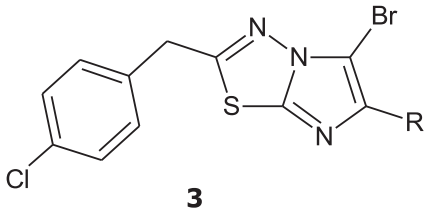 **3**	4-F-ph	a	$C_{17}H_{10}BrClFN_3S$	422.70	155–157
	4-Cl-ph	b	$C_{17}H_{10}BrCl_2N_3S$	439.16	143–145
	4-Br-ph	c	$C_{17}H_{10}Br_2ClN_3S$	483.61	134–137
	4-OCH_3-ph	d	$C_{18}H_{13}BrClN_3OS$	434.74	126–128
	4-CH_3-ph	e	$C_{18}H_{13}BrClN_3S$	418.74	131–133
	2,4-di-Cl-ph	f	$C_{17}H_9BrCl_3N_3S$	473.60	105–107
	Ph	g	$C_{17}H_{11}BrClN_3S$	404.71	149–152
	4-NO_2-ph	h	$C_{17}H_{10}BrClN_4O_2S$	449.71	158–160
	Coumarin-3-yl	i	$C_{20}H_{11}BrClN_3O_2S$	472.74	208–210
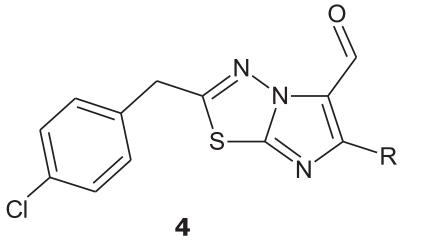 **4**	4-F-ph	a	$C_{18}H_{11}ClFN_3OS$	371.82	138–140
	4-Cl-ph	b	$C_{18}H_{11}Cl_2N_3OS$	388.27	118–120
	4-Br-ph	c	$C_{18}H_{11}BrClN_3OS$	432.72	129–131
	4-OCH_3-ph	d	$C_{19}H_{14}ClN_3O_2S$	383.85	118–121
	4-CH_3-ph	e	$C_{19}H_{14}ClN_3OS$	367.85	83–85
	2,4-di-Cl-ph	f	$C_{18}H_{10}Cl_3N_3OS$	422.72	127–129
	Ph	g	$C_{18}H_{12}ClN_3OS$	353.83	119–121
	4-NO_2-ph	h	$C_{18}H_{11}ClN_4O_3S$	398.82	157–159
	Coumarin-3-yl	i	$C_{21}H_{12}ClN_3O_3S$	421.86	130–133
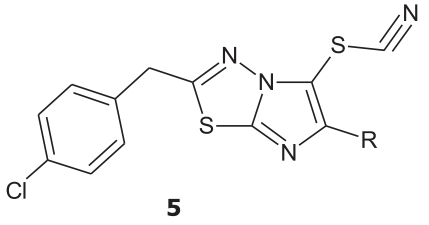 **5**	4-F-ph	a	$C_{18}H_{10}ClFN_4S_2$	400.88	148–150
	4-Cl-p	b	$C_{18}H_{10}Cl2N_4S_2$	417.33	181–183
	4-Br-ph	c	$C_{18}H_{10}BrClN_4S_2$	461.79	181–183
	4-OCH_3-ph	d	$C_{19}H_{13}ClN_4OS_2$	412.92	151–153
	4-CH_3-ph	e	$C_{19}H_{13}ClN_4S_2$	396.92	155–157
	2,4-di-Cl-ph	f	$C_{18}H_9Cl_3N_4S_2$	451.78	130–132
	Ph	g	$C_{18}H_{11}ClN_4S_2$	382.89	121–123
	4-NO_2-ph	h	$C_{18}H_{10}ClN_5O_2S_2$	427.89	167–169
	Coumarin-3-yl	i	$C_{21}H_{11}ClN_4O_2S_2$	450.92	196–198

Results showed that although both molecules induced cytotoxicity in the leukemic cells, **4i** was more potent. **5i** exhibited cytotoxic effects on both REH and K562 cells, when analyzed using trypan blue and MTT assays (Fig. 1A–D), with an IC_{50} value of ~6 and ~3 μM. In contrast, **4i** showed maximum cytotoxic effect on REH cells with an IC_{50} value of ~700 nM (Fig. 1E and F), while in K562 cells, it showed an IC_{50} of ~900 nM (Fig. 1G and H).

3.2.3. *4i and 5i induce cell death without affecting cell cycle progression*

Flow cytometric analysis of the effects of **4i** and **5i** (0.1, 0.5 and 1 μM) on REH cells did not show any cell cycle arrest. Besides, in the case of **5i**, the concentrations used did not exhibit any effect on cell cycle progression (Fig. 2A and B). In contrast, **4i** showed maximum effect resulting in the accumulation of dead cells in the sub G1 phase (Fig. 2C and D). These results thus suggested that **4i** and **5i** induced cell death, without causing cell cycle arrest.

3.2.4. *Effect of 4i on intracellular ROS production*

Production of reactive oxygen species after treatment with drugs is one of the important mediators of cell death [5]. Since we found that **4i** is more potent than **5i**, we have used **4i** to test its ability to induce reactive oxygen species (ROS). Results showed no ROS generation after treatment of **4i** (1 μM), when analyzed after 5, 15, 30 and 60 min, while a positive control showed robust ROS production (Fig. 3). Hence, our data suggested production of ROS is not involved during **4i**-mediated activation of cell death (Fig. 3).

3.2.5. *DNA fragmentation assay*

Internucleosomal cleavage of DNA is one of the hallmarks of apoptosis and cell death. Hence, we wondered whether **4i** treatment can induce DNA fragmentation, as described earlier [1]. The data showed formation of fragmented DNA ladders from 0.5 μM onwards of **4i** treatment (Fig. 4). This suggested that **4i** treatment resulted in DNA fragmentation indicating apoptosis.

3.2.6. *4i treatment results in activation of apoptosis*

To check whether treatment with **4i** induces apoptosis or necrosis, we have stained REH cells treated with **4i** (1 μM) with propidium iodide and Annexin V-FITC antibody, and subjected it to flow cytometric analysis. Results showed a higher amount of annexin-positive cells in the case of **4i** treated REH cells compared

Table 2
Inhibitory effects of compounds on the proliferation of murine leukemia cells (L1210) and human T-lymphocyte cells (CEM) and human cervix carcinoma cells (HeLa).

Compound	IC_{50}[a] (μM)		
	L1210	CEM	HeLa
2a	>250	>250	>250
2b	>250	>250	95 ± 12
2c	>250	>250	>250
2d	38 ± 5	>250	>250
2e	>250	>250	>250
2f	247 ± 4	≥250	109 ± 8
2g	>250	>250	>250
2h	214 ± 23	>250	>250
2i[b]	>10	>10	>10
3a	>250	>250	>250
3b	>250	>250	>250
3c	≥250	238 ± 18	188 ± 11
3d	63 ± 1	58 ± 14	66 ± 12
3e	≥250	>250	>250
3f	31 ± 2	106 ± 5	118 ± 43
3g	≥250	>250	>250
3h	94 ± 24	73 ± 4	≥250
3i	5.2 ± 0.2	3.7 ± 0.9	4.5 ± 0.6
4a	20 ± 2	17 ± 2	20 ± 0
4b	15 ± 5	5.8 ± 0.4	16 ± 2
4c	4.6 ± 0.2	4.0 ± 0.5	4.2 ± 0.6
4d	5.3 ± 0.3	3.8 ± 0.1	6.0 ± 1.0
4e	23 ± 2	17 ± 1	21 ± 1
4f	82 ± 7	79 ± 7	64 ± 2
4g	20 ± 2	22 ± 6	45 ± 16
4h	15 ± 2	13 ± 2	17 ± 0
4i	0.89 ± 0.29	0.75 ± 0.10	0.90 ± 0.08
5a	23 ± 4	24 ± 3	20 ± 0
5b	49 ± 25	30 ± 12	20 ± 2
5c	81 ± 13	61 ± 18	22 ± 3
5d	16 ± 4	10 ± 2	9.0 ± 5.0
5e	32 ± 2	22 ± 2	22 ± 0
5f	49 ± 12	46 ± 19	18 ± 1
5g	24 ± 6	14 ± 4	12 ± 8
5h	50 ± 12	20 ± 6	16 ± 1
5i	1.3 ± 0.0	1.4 ± 0.4	1.0 ± 0.0
Melphalan	2.13 ± 0.02	1.4 ± 0.4	NT
Levamisole	206 ± 6	>250	≥250

[a] 50% inhibitory concentration.
[b] No dose–response at higher concentration.

Table 3
Inhibitory effects of compounds on the proliferation of REH and K562 cell lines.

Compound	IC_{50}[a] (μM)	
	REH	K562
4i	0.67	0.9
5i	6.20	3.1

[a] 50% inhibitory concentration.

to the control (Fig. 5). A significant increase in the number of apoptotic cells was seen (Fig. 5). These results suggest that **4i** may induce apoptosis as a major cause of cell death in REH cells.

3.2.7. *4i treatment results in the loss of the mitochondrial membrane potential*

Mitochondria play a major role in the activation of apoptosis and loss of mitochondrial membrane potential is one of the well-studied aspects during induction of apoptosis [6]. Thus, we checked for the changes in mitochondrial membrane potential after treatment of REH cells with **4i** (Fig. 6A and B). Results showed a significant reduction in mitochondrial membrane potential at the tested concentrations of **4i**, which suggests that the loss of mitochondrial membrane potential is one of the key events leading to cell death by **4i**. This further indicates that activation of an intrinsic pathway of apoptosis could be responsible during **4i**-mediated apoptosis.

3.2.8. *Effect of 4i treatment is robust in cancerous cells compared to normal cells*

To investigate the effect of **4i** on cancerous versus normal cells, we treated REH and 293T cells with 0.5 μM of **4i** and performed live dead assay using ethidium bromide stain at 48 h time point. Results showed that **4i** is more cytotoxic against REH cells (~6 fold) compared to 293T normal cells (Suppl. Fig. 4A and B). This suggests that **4i** could effectively kill the cells with high proliferation rate which is a characteristic feature of cancerous cells.

4. Conclusions

In summary, a series of 36 derivatives with various structural features on imidazo[2,1-*b*][1,3,4]thiadiazoles were synthesized and their cytotoxicity evaluation was performed against human cervix carcinoma HeLa, T-lymphocyte CEM, as well as murine leukemia L1210 cells. Our structure activity relationship studies indicated that, formyl (**4c**, **4d** & **4i**) and thiocyanate (**5a**, **5d**, **5g** & **5i**) substituents are required for good cytotoxicity activity. Replacements of the phenyl group at the 6th position by coumarin produced more cytotoxic derivatives (**3i**, **4i** & **5i**). Therefore derivative **4i** was selected for further study to understand the mechanism of action against REH and K562 cells. The cell cycle study, analysis of mitochondrial membrane potential, DNA fragmentation and Annexin V-FITC staining suggested that **4i** was able to induce apoptosis without arresting cell cycle.

5. Experimental section

5.1. Chemicals and reagents

The melting points are uncorrected. Silica gel plates were used for TLC by using $CHCl_3$/MeOH in various proportions. The IR spectra were recorded in KBr on a Jasco 430+; the ^1H NMR spectra were recorded in $CDCl_3$/DMSO on a Bruker (400 MHz), and *J* values were reported in hertz (Hz). Mass spectra were recorded in triple quadrapole LCMS-6410 from Agilent technologies. Phenacyl bromide [7], 4-chlorophenacyl bromide [8], 4-bromophenacyl bromide [9], 4-methoxyphenacyl bromide [10], 4-methylphenacyl bromide [11], 2,4-dichlorophenacyl bromide [12], 4-fluorophenacyl bromide [13], 4-nitrophenacyl bromide [14], 3-(bromoacetyl)-2H-chromen-2-one [15], 2-amino-5-(4-chlorobenzyl)-1,3,4-thiadiazole **1**, **2a**, **3a**, **4a** and **5a** were prepared according to the literature [1]. Compounds **2b**, **2c**, **2e** and **2h** have been previously reported [16].

5.2. General procedure for the synthesis of the imidazo[2,1-b][1,3,4] thiadiazoles (*2d*, *2f*, *2g* and *2i*)

The 2-amino-5-(4-chlorobenzyl)-1,3,4-thiadiazole **1** (30 mmol) was treated with the respective phenacyl bromide (30 mmol), in ethanol (150 mL). The mixture was refluxed for 10–12 h. Excess of solvent was removed under reduced pressure and the solid hydrobromide was separated by filtration, washed with cold ethanol and dried. Neutralization of hydrobromide salts with cold aqueous solution of sodium carbonate yielded the corresponding free base which was filtered with a yield of 50–65%.

5.2.1. *2-(4-Chlorobenzyl)-6-(4-methoxyphenyl)imidazo[2,1-b] [1,3,4]thiadiazole (2d)*

Obtained according to the general procedure for the synthesis of the imidazo[2,1-*b*][1,3,4]thiadiazole-Yield 6.405 g, 60%, FT-IR (KBr,

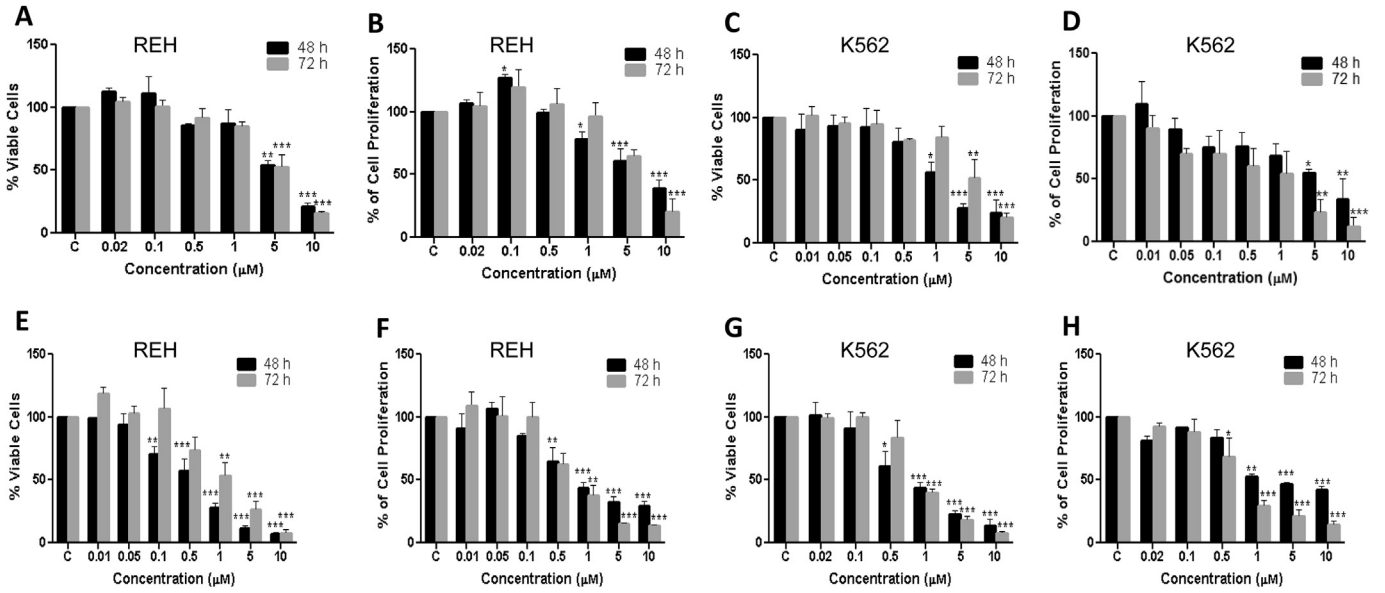

Fig. 1. Cytotoxic effect of 4i and 5i on REH and K562 cells. REH and K562 cells were treated with increasing concentration of **4i** and **5i** (0–10 μM). Trypan blue assay and MTT assays were performed at 48 and 72 h of treatment with compound. A. Trypan blue assay for **5i**-treated REH cells. B. MTT assay for **5i**-treated REH cells. C. Trypan blue assay for **5i**-treated K562 cells. D. MTT assay for **5i**-treated K562 cells. E. Trypan blue assay for **4i**-treated REH cells. F. MTT assay for **4i**-treated REH cells. G. Trypan blue assay for **4i**-treated K562 cells. H. MTT assay for **4i**-treated K562 cells. The cells treated with highest concentration of DMSO used in the study served as vehicle control. In all the panels 'C' indicates, DMSO treated control and error bar was plotted based on three independent experiments.

cm^{-1}): 3146, 3041, 2939, 2842, 1537, 1481, 1251, 1181, 1093, 1025, 837. NMR (400 MHz, DMSO-d_6) δ 3.84 (s, 3H, $-OCH_3$), 4.26 (s, 2H), 6.92 (d, $J = 8$ Hz, 2H), 7.27 (d, $J = 8$ Hz, 2H), 7.36 (d, $J = 8$ Hz, 2H), 7.73 (d, $J = 8$ Hz, 2H), 7.88 (s, 1H). MS (ESI) *m/z*: 356.0 (355.8).

5.2.2. (2-(4-Chlorobenzyl)-6-(2,4-dichlorophenyl)imidazo[2,1-b][1,3,4] thiadiazole (**2f**)

Obtained according to the general procedure for the synthesis of the imidazo[2,1-*b*][1,3,4]thiadiazole-Yield 5.920 g, 50%, FT-IR (KBr, cm^{-1}): 3185, 3072, 2924, 1584, 1483, 1379, 1286, 1099, 873. NMR (400 MHz, DMSO-d_6) δ 4.28 (s, 2H), 7.28 (d, $J = 8$ Hz, 2H), 7.30–7.33 (m, 1H), 7.37 (d, $J = 8$ Hz, 2H), 7.46 (m, 1H), 8.09 (d, $J = 8.8$ Hz, 1H), 8.38 (s, 1H). MS (ESI) *m/z*: 395.9 (394.7).

5.2.3. 2-(4-Chlorobenzyl)-6-phenylimidazo[2,1-b][1,3,4]thiadiazole (**2g**)

Obtained according to the general procedure for the synthesis of the imidazo[2,1-*b*][1,3,4]thiadiazole-Yield 6.353 g, 65%, FT-IR (KBr, cm^{-1}): 3101, 3068, 2941, 2910, 1528, 1483, 1435, 1193, 1020. NMR (400 MHz, DMSO-d_6) δ 4.27 (s, 2H), 7.25–7.31 (m, 3H, ar), 7.34–7.42 (m, 4H, ar), 7.80 (d, $J = 8$ Hz, 2H), 7.97 (s, 1H). MS (ESI) *m/z*: 326.40 (325.82).

5.2.4. 3-[2-(4-Chlorobenzyl)imidazo[2,1-b][1,3,4]thiadiazol-6-yl]-2H-chromen-2-one (**2i**)

Obtained according to the general procedure for the synthesis of the imidazo[2,1-*b*][1,3,4]thiadiazole-Yield 5.907 g, 50%, FT-IR (KBr, cm^{-1}): 3145, 3052, 2973, 1729, 1609, 1484, 1102, 1004, 925. NMR (400 MHz, DMSO-d_6) δ 4.48 (s, 2H), 7.38 (t, $J = 16$ Hz, 1H), 7.45–7.46 (m, 5H), 7.61 (t, $J = 16$ Hz, 1H), 7.87 (d, $J = 8$ Hz, 1H), 8.56 (s, 1H), 8.66 (s, 1H). MS (ESI) *m/z*: 392.0 (393.9).

5.3. General procedure for the preparation of the 5-bromo-imidazo[2,1-b][1,3,4]thiadiazole derivatives (**3b**–**i**)

To the respective imidazo[2,1-*b*][1,3,4]thiadiazole (5 mmol) **2**, sodium acetate (10 mmol) and 10 mL of glacial acetic acid stirred together at room temperature was added dropwise bromine (6 mmol). After the addition, stirring was continued for 30 min. The mixture was poured into 100 mL of water from which a solid separated. The solid was collected by filtration and washed with water, dried and crystallized from EtOH–$CHCl_3$ with a yield of 60–85%.

5.3.1. 5-Bromo-2-(4-chlorobenzyl)-6-(4-chlorophenyl)imidazo[2,1-b][1,3,4] thiadiazole (**3b**)

Obtained according to the general procedure for the synthesis of the 5-bromo-imidazo[2,1-*b*][1,3,4]thiadiazole-Yield 1.865 g, 85%, FT-IR (KBr, cm^{-1}): 3044, 2953, 2925, 1484, 1401, 1322, 1090, 824. NMR (400 MHz, DMSO-d_6) δ 4.32 (s, 2H), 7.28 (d, $J = 8.8$ Hz, 2H), 7.38 (d, $J = 8.8$ Hz, 2H), 7.41 (d, $J = 8.8$ Hz, 2H),7.95 (d, $J = 8.8$ Hz, 2H). MS (ESI) *m/z*: 439.9 (439.2).

5.3.2. 5-Bromo-6-(4-bromophenyl)-2-(4-chlorobenzyl)imidazo[2,1-b][1,3,4] thiadiazole (**3c**)

Obtained according to the general procedure for the synthesis of the 5-bromo-imidazo[2,1-*b*][1,3,4]thiadiazole-Yield 1.934 g, 80%, FT-IR (KBr, cm^{-1}): 3085, 2925, 1586, 1483, 1399, 1320, 1092, 832. NMR (400 MHz, DMSO-d_6) δ 4.50 (s, 2H), 7.44 (s, 4H), 7.67 (d, $J = 8$ Hz, 2H), 7.90 (d, $J = 8$ Hz, 2H). MS (ESI) *m/z*: 481.8 (483.6).

5.3.3. 5-Bromo-2-(4-chlorobenzyl)-6-(4-methoxyphenyl)imidazo[2,1-b][1,3,4] thiadiazole (**3d**)

Obtained according to the general procedure for the synthesis of the 5-bromo-imidazo[2,1-*b*][1,3,4]thiadiazole-Yield 1.738 g, 80%, FT-IR (KBr, cm^{-1}): 3075, 3004, 2937, 2840, 1608, 1531, 1479, 1254, 1177, 1026, 826. NMR (400 MHz, DMSO-d_6) δ 3.78 (s, 3H, $-OCH_3$), 4.49 (s, 2H, $-CH_2-$), 7.03 (d, $J = 8$ Hz, 2H), 7.44 (s, 4H), 7.87 (d, $J = 8$ Hz, 2H). MS (ESI) *m/z*: 433.90 (434.74).

5.3.4. 5-Bromo-2-(4-chlorobenzyl)-6-(4-methylphenyl)imidazo[2,1-b][1,3,4] thiadiazole (**3e**)

Obtained according to the general procedure for the synthesis of the 5-bromo-imidazo[2,1-*b*][1,3,4]thiadiazole-Yield 1.570 g, 75%,

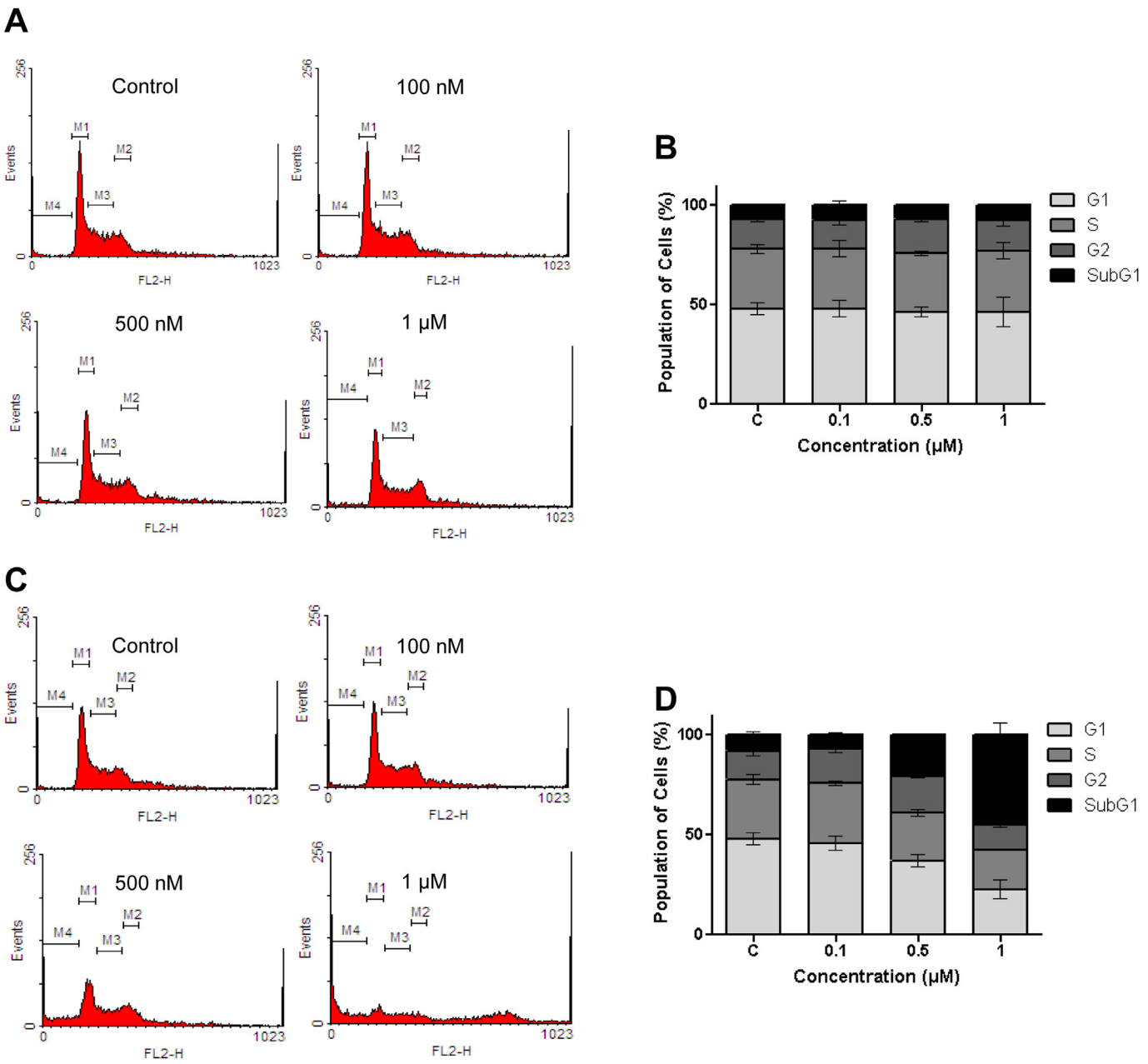

Fig. 2. Effect of 4i and 5i on cell cycle progression. REH cells were treated with **4i** and **5i** (0, 0.1, 0.5 and 1 μM). After 48 h of treatment, cells were harvested, fixed, stained with propidium iodide and analyzed using a flow cytometer. A. Histogram representing effect of **5i** on cell cycle progression. B. Bar diagram representing distribution of cells at different phases of cell cycle following treatment with **5i**. C. Histogram representing effect of **4i** on cell cycle in REH cells. D. Bar diagram representing distribution of cells at different phases of cell cycle following treatment with **4i**. In both panels, B and D error bars shown were based on two independent experiments.

FT-IR (KBr, cm^{-1}): 3027, 2919, 1471, 1333, 1097, 1022, 823. NMR (400 MHz, DMSO-d_6) δ 2.32 (s, 3H, CH_3), 4.49 (s, 2H), 7.27 (d, $J = 8$ Hz, 2H), 7.44 (s, 4H), 7.84 (d, $J = 8$ Hz, 2H). MS (ESI) m/z : 419.9 (418.7).

*5.3.5. 5-Bromo-2-(4-chlorobenzyl)-6-(2,4-dichlorophenyl)imidazo [2,1-b][1,3,4] thiadiazole (**3f**)*

Obtained according to the general procedure for the synthesis of the 5-bromo-imidazo[2,1-*b*][1,3,4]thiadiazole-Yield 1.657 g, 70%,FT-IR (KBr, cm^{-1}): 3086, 3029, 2920, 1529, 1467, 1416, 1100, 820. NMR (400 MHz, DMSO-d_6) δ 4.52 (s, 2H), 7.45 (s, 4H), 7.53 (m, 2H), 7.76 (s, 1H). MS (ESI) m/z : 471.8 (473.6).

*5.3.6. 5-Bromo-2-(4-chlorobenzyl)-6-phenylimidazo[2,1-b][1,3,4] thiadiazole (**3g**)*

Obtained according to the general procedure for the synthesis of the 5-bromo-imidazo[2,1-*b*][1,3,4]thiadiazole-Yield 1.659 g, 82%, FT-IR (KBr, cm^{-1}): 3060, 3026, 2927, 1598, 1481, 1433, 1323, 1084, 1010. NMR (400 MHz, DMSO-d_6) δ 4.50 (s, 2H), 7.33–7.37 (m, 1H), 7.44–7.48 (m, 6H), 7.93 (d, $J = 7.2$ Hz, 2H). MS (ESI) m/z: 405.9 (404.7).

*5.3.7. 5-Bromo-2-(4-chlorobenzyl)-6-(4-nitrophenyl)imidazo[2,1-b][1,3,4] thiadiazole (**3h**)*

Obtained according to the general procedure for the synthesis of the 5-bromo-imidazo[2,1-*b*][1,3,4]thiadiazole-Yield 1.753 g, 78%, FT-IR (KBr, cm^{-1}): 3081, 2924, 2824, 1598, 1520, 1343, 1100, 857.

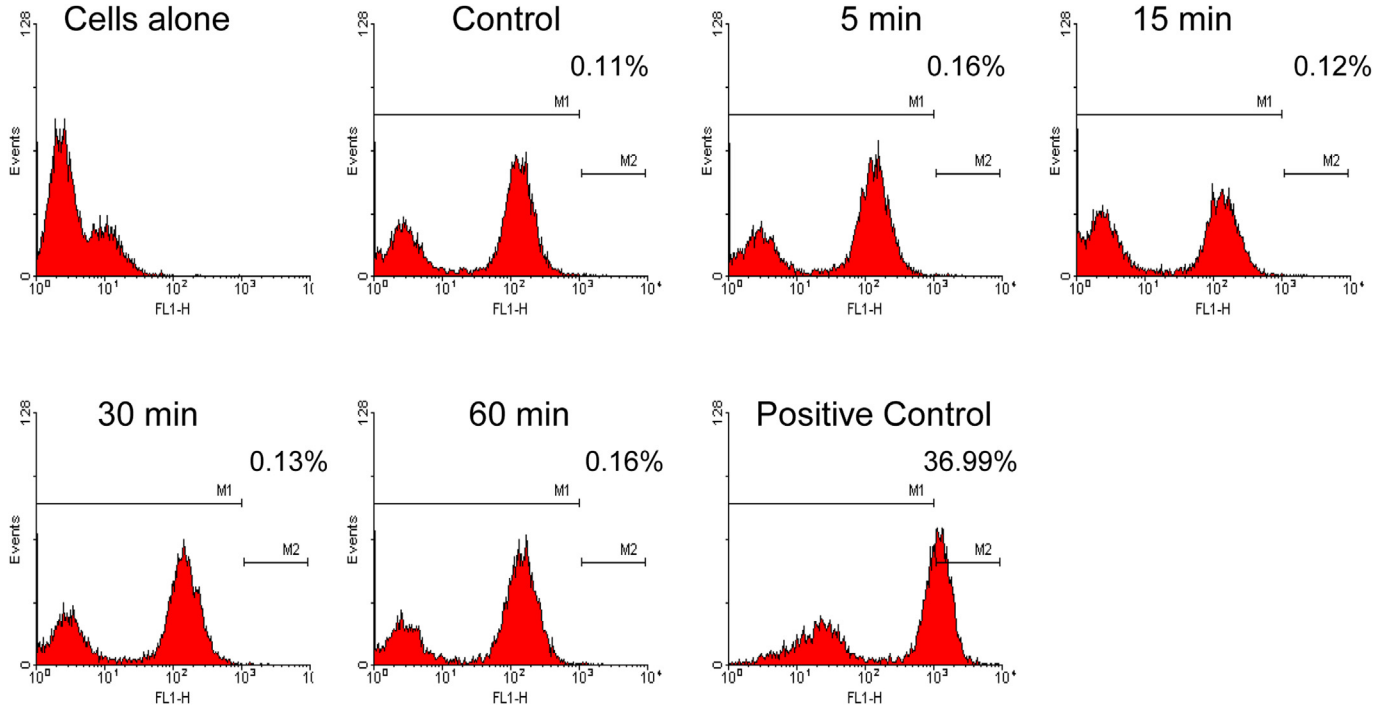

Fig. 3. Detection of intracellular ROS production in REH cells following treatment with 4i. REH cells treated with 1 μM of **4i** for different time periods (5, 15, 30 and 60 min), cells were harvested, washed and stained with H_2DCFDA (0.5 μM) for 15 min at 37 °C. ROS production was analyzed using flow cytometry. H_2O_2 treated cells were used as a positive control, while untreated cells served as a negative control. Cells treated with H_2DCFDA served as control for the study. The percent of cells which were positive for fluorescent ROS were indicated.

NMR (400 MHz, DMSO-d_6) δ 4.52 (s, 2H), 7.45 (s, 4H), 8.24 (d, J = 8 Hz, 2H), 8.34 (d, J = 8 Hz, 2H). MS (ESI) m/z: 448.8 (449.7).

*5.3.8. 3-[5-Bromo-2-(4-chlorobenzyl)imidazo[2,1-b][1,3,4] thiadiazol-6-yl]-2H-chromen-2-one (**3i**)*

Obtained according to the general procedure for the synthesis of the 5-bromoimidazo[2,1-*b*][1,3,4]thiadiazole-Yield 1.607 g, 68%, FT-IR (KBr, cm^{-1}): 3095, 2935, 2829, 1591, 1522, 1334, 1101, 862. NMR (400 MHz, DMSO-d_6) δ 4.54 (s, 2H), 7.43–7.39 (m, 1H), 7.48–7.46 (m, 5H), 7.70–7.65 (m, 1H), 7.87–7.83 (m, 1H), 8.33 (s, 1H). MS (ESI) m/z: 471.9 (472.7).

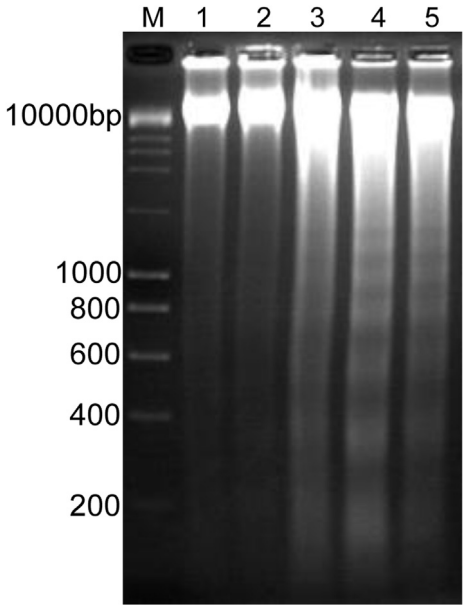

Fig. 4. Evaluation of effect of 4i by DNA fragmentation assay. REH cells were treated with 0, 0.1, 0.5,1 and 5 μM of **4i** for 48 h, genomic DNA was isolated using non-denaturing protocol and analyzed by agarose gel electrophoresis (2%). Lane 1 represents the DMSO control, Lanes 2, 3, 4 and 5 represents cells treated with 0.1, 0.5, 1 and 5 μM of **4i**, respectively. 'M' represents the marker lane.

*5.4. General procedure for the preparation of the imidazo[2,1-b] [1,3,4]thiadiazole-5-carbaldehydes (**4b**–**i**)*

The Vilsmeier reagent was prepared at 0–5 °C by dropping $POCl_3$ (2.3 g, 15 mmol) into a stirred solution of DMF (10 mL). The respective imidazo[2,1-*b*][1,3,4]thiadiazole **2** (4 mmol) was added slowly to the Vilsmeier reagent while maintaining stirring and cooling for 2 h. Further stirring was continued for 6 h at 80–90 °C. The resulting reaction mixture was poured into 100 mL of water; the precipitate was filtered, pressed, suspended in water and neutralized to pH 7 with cold aqueous solution of sodium carbonate. The solid was separated by filtration, washed with water, dried and crystallized from EtOH with a yield of 45–58%.

*5.4.1. 2-(4-Chlorobenzyl)-6-(4-chlorophenyl)imidazo[2,1-b][1,3,4] thiadiazole-5-carbaldehyde (**4b**)*

Obtained according to the general procedure for the synthesis of the imidazo[2,1-*b*][1,3,4]thiadiazole-5-carbaldehyde-Yield 0.854 g, 55%, FT-IR (KBr, cm^{-1}): 3071, 3028, 2954, 2914, 1670, 1477, 1312, 1193, 1027, 824. NMR (400 MHz, DMSO-d_6) δ 4.42 (s, 2H), 7.30 (d, J = 8 Hz, 2H), 7.39 (d, J = 8 Hz, 2H), 7.49 (d, J = 8 Hz, 2H), 7.84 (d, J = 8 Hz, 2H), 10.08 (s, 1H, –CHO). MS (ESI) m/z: 386.0 (388.3).

*5.4.2. 6-(4-Bromophenyl)-2-(4-chlorobenzyl)imidazo[2,1-b][1,3,4] thiadiazole-5-carbaldehyde (**4c**)*

Obtained according to the general procedure for the synthesis of the imidazo[2,1-*b*][1,3,4]thiadiazole-5-carbaldehyde-Yield 0.865 g,

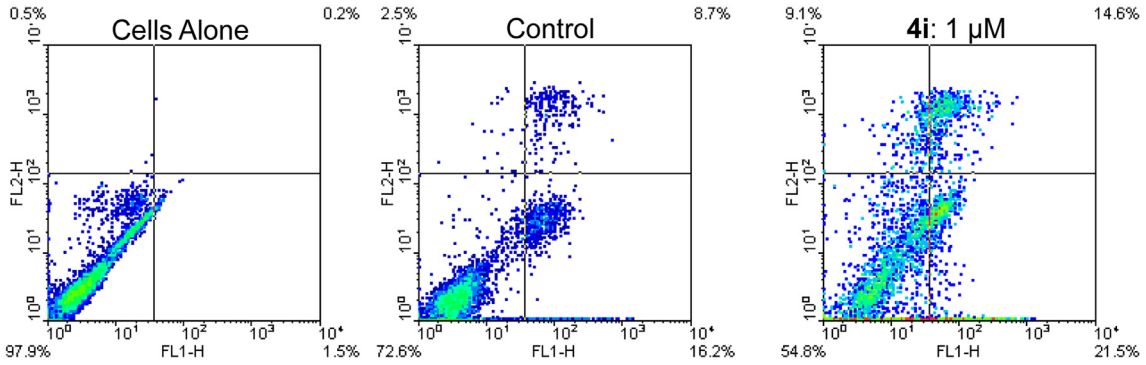

Fig. 5. Annexin V-FITC flow cytometry. The mobilization of phosphatidylserine from inner membrane to outer membrane was detected using Annexin V-FITC staining. After 48 h of treatment with **4i** (1 μM) cells were harvested, and stained with Annexin V-FITC and propidium iodide, and analyzed in a flow cytometer. DMSO treated cells were used as vehicle control. Density plot represent control and treated cells.

50%, FT-IR (KBr, cm^{-1}): 3092, 3043, 2928, 2859, 1671, 1484, 1308, 1095, 1014. NMR (400 MHz, DMSO-d_6) δ 4.55 (s, 2H), 7.44 (s, 4H), 7.69 (d, $J = 8$ Hz, 2H), 7.91 (d, $J = 8$ Hz, 2H), 9.97 (s, 1H, −CHO). MS (ESI) *m/z*: 431.9 (432.7).

*5.4.3. 2-(4-Chlorobenzyl)-6-(4-methoxyphenyl)imidazo[2,1-b][1,3,4]thiadiazole-5-carbaldehyde (**4d**)*

Obtained according to the general procedure for the synthesis of the imidazo[2,1-*b*][1,3,4]thiadiazole-5-carbaldehyde-Yield 0.767 g, 50%, FT-IR (KBr, cm^{-1}): 3079, 3034, 2929, 2861, 1675, 1489, 1311, 1099, 1010. NMR (400 MHz, DMSO-d_6) δ 3.82 (s, 3H, $-OCH_3$), 4.55 (s, 2H, $-CH_2-$), 7.07 (d, $J = 8$ Hz, 2H), 7.45 (s, 4H), 7.92 (d, $J = 8$ Hz, 2H), 9.95 (s, 1H, −CHO). MS (ESI) *m/z*: 383.85 (382.30).

*5.4.4. 2-(4-Chlorobenzyl)-6-(4-methylphenyl)imidazo[2,1-b][1,3,4]thiadiazole-5-carbaldehyde (**4e**)*

Obtained according to the general procedure for the synthesis of the imidazo[2,1-*b*][1,3,4]thiadiazole-5-carbaldehyde-Yield 0.765 g, 52%, FT-IR (KBr, cm^{-1}): 3033, 2922, 2852, 1664, 1486, 1390, 1326, 1096, 1019, 829. NMR (400 MHz, DMSO-d_6) δ 2.34 (s, 3H, $-CH_3$), 4.55 (s, 2H), 7.32 (d, $J = 8$ Hz, 2H), 7.46 (s, 4H), 7.82 (d, $J = 8$ Hz, 2H), 9.94 (s, 1H, −CHO). MS (ESI) *m/z*: 366.0 (367.9).

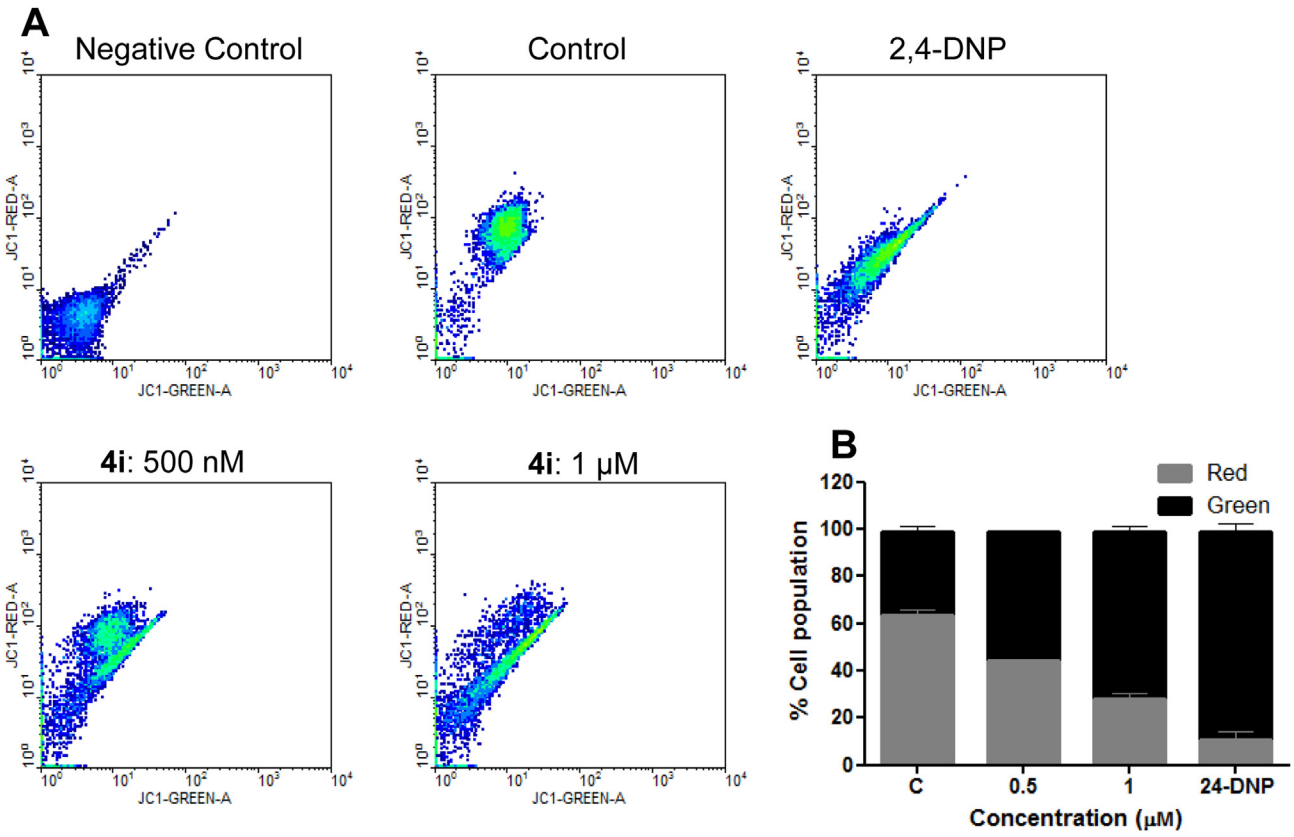

Fig. 6. Measurement of mitochondrial membrane potential. Total mitochondrial membrane potential was measured after treatment of **4i** with REH cells (0.5 and 1 μM for 48 h). Following harvesting, cells were treated with JC-1 at 37 °C for 20 min and analyzed in a flow cytometer. 2,4-DNP was used as positive control, negative control indicates DMSO-treated cells without JC-1 staining and Control indicates JC-1 stained DMSO treated cells. A. Density plot showing JC1 staining of control and treated cells. B. Bar diagram showing red and green fluorescence ratio. (For interpretation of the references to color in this figure legend, the reader is referred to the web version of this article.)

*5.4.5. 2-(4-Chlorobenzyl)-6-(2,4-dichlorophenyl)imidazo[2,1-b][1,3,4] thiadiazole-5-carbaldehyde (**4f**)*

Obtained according to the general procedure for the synthesis of the imidazo[2,1-*b*][1,3,4]thiadiazole-5-carbaldehyde-Yield 0.913 g, 54%, FT-IR (KBr, cm^{-1}): 3085, 3041, 2928, 2865, 1669, 1489, 1315, 1101, 1015. NMR ^1H (400 MHz, DMSO-d_6) δ 4.44 (s, 2H), 7.31–7.29 (m, 2H), 7.40–7.37 (m, 2H), 7.50–7.48 (d, $J = 8$ Hz, 2H), 7.57 (m, 1H, ar), 9.77 (s, 1H, CHO). MS (ESI) *m*/*z*: 422.40 (422.72). ^{13}C 176.92 (s), 166.93 (s), 134.47 (s), 133.25 (s), 133.18 (s), 130.42 (s), 130.22 (s), 129.60 (s), 127.44 (s), 37.67 (s). MS (ESI) *m*/*z*: 422.40 (422.72).

*5.4.6. 2-(4-Chlorobenzyl)-6-phenylimidazo[2,1-b][1,3,4] thiadiazole-5-carbalde hyde (**4g**)*

Obtained according to the general procedure for the synthesis of the imidazo[2,1-*b*][1,3,4]thiadiazole-5-carbaldehyde-Yield 0.820 g, 58%, FT-IR (KBr, cm^{-1}): 3070, 2970, 2927, 2859, 1672, 1484, 1443, 1337, 1185, 1086, 846. NMR (400 MHz, DMSO-d_6) δ 4.56 (s, 2H), 7.48 (s, 4H), 7.49–7.53 (m, 3H), 7.91–7.93 (m, 2H), 9.96 (s, 1H, –CHO). MS (ESI) *m*/*z*: 352.0 (353.8).

*5.4.7. 2-(4-Chlorobenzyl)-6-(4-nitrophenyl)imidazo[2,1-b][1,3,4] thiadiazole-5-carbaldehyde (**4h**)*

Obtained according to the general procedure for the synthesis of the imidazo[2,1-*b*][1,3,4]thiadiazole-5-carbaldehyde-Yield 0.925 g, 58%, FT-IR (KBr, cm^{-1}): 3092, 2935, 2849, 1670, 1599, 1520, 1343, 1102, 856. NMR (400 MHz, DMSO-d_6) δ 4.57 (s, 2H), 7.45 (s, 4H), 8.26 (d, $J = 8$ Hz, 2H), 8.34 (d, $J = 8$ Hz, 2H), 10.06 (s, 1H, –CHO). MS (ESI) *m*/*z*: 397.0 (398.8).

*5.4.8. 2-(4-Chlorobenzyl)-6-(2-oxo-2H-chromen-3-yl)imidazo[2,1-b][1,3,4] thiadiazole-5-carbaldehyde (**4i**)*

Obtained according to the general procedure for the synthesis of the imidazo[2,1-*b*][1,3,4]thiadiazole-5-carbaldehyde-Yield 0.843 g, 50%, FT-IR (KBr, cm^{-1}): 3040, 2914, 1722, 1668, 1611, 1483, 1368, 1315, 1052. NMR (400 MHz, DMSO-d_6) δ 4.57 (s, 2H), 7.39–7.50 (m, 6H), 7.67–7.71 (m, 1H), 7.87–7.89 (m, 1H), 8.51 (s, 1H), 9.99 (s, 1H, –CHO). MS (ESI) *m*/*z*: 419.9 (421.9).

*5.5. General procedure for the preparation of the imidazo[2,1-b][1,3,4]thiadiazol-5-yl-thiocyanates (**5b**–**i**)*

To a mixture of imidazo[2,1-*b*][1,3,4]thiadiazole **2** (10 mmol) and potassium thiocyanate (1.56 g, 16 mmol) in glacial acetic acid (50 mL) was added bromine (1.6 g, 10 mmol) in glacial acetic acid (20 mL) at 0–5 °C dropwise with stirring. Stirring was continued for 30 min at 15–20 °C and then at room temperature for 1 h. The reaction mixture was poured into ice water, filtered, washed with water and crystallized from EtOH–$CHCl_3$ with a yield of 50–57%.

*5.5.1. 2-(4-Chlorobenzyl)-6-(4-chlorophenyl)imidazo[2,1-b][1,3,4] thiadiazol-5-yl thiocyanate (**5b**)*

Obtained according to the general procedure for the synthesis of the imidazo[2,1-*b*][1,3,4]thiadiazole-5-carbaldehyde-Yield 0.225 g, 54%, FT-IR (KBr, cm^{-1}): 3065, 2921, 2850, 2161, 1462, 1096, 832. NMR (400 MHz, DMSO-d_6) δ 4.38 (s, 2H), 7.31 (d, $J = 8.4$ Hz, 2H), 7.40 (d, $J = 8.8$ Hz, 2H), 7.48 (d, $J = 8.8$ Hz, 2H), 7.92 (d, $J = 8.4$ Hz, 2H). MS (ESI) *m*/*z*: 416.8 (417.3).

*5.5.2. 6-(4-Bromophenyl)-2-(4-chlorobenzyl)imidazo[2,1-b][1,3,4] thiadiazol-5-yl thiocyanate (**5c**)*

Obtained according to the general procedure for the synthesis of the imidazo[2,1-*b*][1,3,4]thiadiazole-5-carbaldehyde-Yield 0.240 g, 52%, FT-IR (KBr, cm^{-1}): 3063, 2924, 2852, 2161, 1673, 1585, 1462, 1398, 1097, 1009, 1271, 831. NMR (400 MHz, DMSO-d_6) δ 4.58 (s, 2H), 7.46 (s, 4H), 7.76 (d, $J = 8$ Hz, 2H), 7.92 (d, $J = 8$ Hz, 2H). MS (ESI) *m*/*z*: 460.9 (461.8).

*5.5.3. 2-(4-Chlorobenzyl)-6-(4-methoxyphenyl)imidazo[2,1-b][1,3,4]thiadiazol-5-yl thiocyanate (**5d**)*

Obtained according to the general procedure for the synthesis of the imidazo[2,1-*b*][1,3,4]thiadiazole-5-carbaldehyde-Yield 0.218 g, 53%, FT-IR (KBr, cm^{-1}): 3007, 2965, 2842, 2154, 1610, 1527, 1480, 1099, 1035, 831. NMR (400 MHz, DMSO-d_6) δ 3.81 (s, 3H, $-OCH_3$), 4.56 (s, 2H), 7.11 (d, $J = 8.8$ Hz, 2H), 7.46 (s, 4H), 7.92 (d, $J = 8.8$ Hz, 2H). MS (ESI) *m*/*z*: 413.0 (412.9).

*5.5.4. 2-(4-Chlorobenzyl)-6-(4-methylphenyl)imidazo[2,1-b][1,3,4] thiadiazol-5-yl thiocyanate (**5e**)*

Obtained according to the general procedure for the synthesis of the imidazo[2,1-*b*][1,3,4]thiadiazole-5-carbaldehyde-Yield 0.214 g, 54%, FT-IR (KBr, cm^{-1}): 3029, 2915, 2157, 1605, 1479, 1325, 1123, 827. NMR (400 MHz, DMSO-d_6) δ 2.36 (s, 3H, $-CH_3$), 4.57 (s, 2H), 7.34 (d, $J = 8$ Hz, 2H), 7.46 (s, 4H), 7.86 (d, $J = 8$ Hz, 2H). MS (ESI) *m*/*z*: 396.30 (396.92).

*5.5.5. 2-(4-Chlorobenzyl)-6-(2,4-dichlorophenyl)imidazo[2,1-b][1,3,4]thiadiazol-5-yl thiocyanate (**5f**)*

Obtained according to the general procedure for the synthesis of the imidazo[2,1-*b*][1,3,4]thiadiazole-5-carbaldehyde-Yield 0.230 g, 51%, FT-IR (KBr, cm^{-1}): 3085, 2920, 2854, 2163, 1586, 1462, 1099, 822. NMR (400 MHz, DMSO-d_6) δ 4.28 (s, 2H), 7.31–7.28 (m, 2H), 7.37–7.35 (m, 2H), 7.46 (m, 1H), 8.09–8.07 (d, $J = 8$ Hz, 1H), (8.39 s, 1H). MS (ESI) *m*/*z*: 450.8 (451.8).

*5.5.6. 2-(4-Chlorobenzyl)-6-phenylimidazo[2,1-b][1,3,4]thiadiazol-5-yl thiocyanate (**5g**)*

Obtained according to the general procedure for the synthesis of the imidazo[2,1-*b*][1,3,4]thiadiazole-5-carbaldehyde-Yield 0.218 g, 57%, FT-IR (KBr, cm^{-1}): 3056, 2923, 2157, 1481, 1441, 1325, 1092, 840. NMR (400 MHz, DMSO-d_6) δ 4.58 (s, 2H), 7.45–7.47 (m, 5H), 7.53 (t, $J = 16$ Hz, 2H), 7.97 (d, $J = 8$ Hz, 2H). MS (ESI) *m*/*z*: 383.0 (382.9).

*5.5.7. 2-(4-Chlorobenzyl)-6-(4-nitrophenyl)imidazo[2,1-b][1,3,4] thiadiazol-5-yl thiocyanate (**5h**)*

Obtained according to the general procedure for the synthesis of the imidazo[2,1-*b*][1,3,4]thiadiazole-5-carbaldehyde-Yield 0.222 g, 52%, FT-IR (KBr, cm^{-1}): 3082, 3036, 2926, 2841, 2160, 1598, 1510, 1407, 1340, 1108, 1012, 854. NMR (400 MHz, DMSO-d_6) δ 4.60 (s, 2H), 7.45–7.47 (s, 4H), 8.26 (d, $J = 8$ Hz, 2H), 8.40 (d, $J = 8$ Hz, 2H). MS (ESI) *m*/*z*: 425.9 (427.9).

*5.5.8. 2-(4-Chlorobenzyl)-6-(2-oxo-2H-chromen-3-yl)imidazo[2,1-b][1,3,4] thiadiazol-5-yl thiocyanate (**5i**)*

Obtained according to the general procedure for the synthesis of the imidazo[2,1-*b*][1,3,4]thiadiazole-5-carbaldehyde-Yield 0.207 g, 46%, FT-IR (KBr, cm^{-1}): 3029, 2941, 1720, 1615, 1479, 1373, 1316, 1063. NMR (400 MHz, DMSO-d_6) δ 4.63 (s, 2H), 7.54–7.42 (m, 6H), 7.75–7.69 (m, 1H), 7.92–7.89 (m, 1H), 8.49 (s, 1H). ^{13}C 166.08 (s), 159.80 (s), 153.93 (s), 148.58 (s), 144.40 (s), 142.95 (s), 134.44 (s), 133.04 (s), 132.63 (s), 130.39 (s), 129.59 (s), 128.66 (s), 125.03 (s), 120.45 (s), 119.78 (s), 108.67 (s), 37.71 (s). MS (ESI) *m*/*z*: 451.00 (450.92).

6. Bioevaluations

6.1. Cell culture

Human cell lines REH (B-cell leukemia), K562 (Chronic myelogenous leukemia), were cultured in RPMI1640 (Sera Lab, UK) and

293T (Human Embryonic Kidney cells) were cultured in DMEM containing 10% FBS (Gibco BRL, USA) along with 100 U of Penicillin G/ml and 100 μg of streptomycin/ml (Sigma–Aldrich, USA) at 37 °C in a humidified atmosphere containing 5% CO_2 [17].

6.1.1. Cytotoxicity in human and murine tumor cell lines

All the compounds in Scheme 1 were evaluated for their cytostatic activity against human HeLa cervix carcinoma cells, human CEM $CD4^+$ T-lymphocytes as well as murine L1210 cells. All assays were performed in 96-well microtiter plates. To each well were added (5–7.5) × 10^4 tumor cells and a given amount of the test compound. The cells were allowed to proliferate for 48 h (murine leukemia L1210 cells) or 72 h (human lymphocytic CEM and human cervix carcinoma HeLa cells) at 37 °C in a humidified CO_2-controlled atmosphere. At the end of the incubation period, the cells were counted in a Coulter counter. The IC_{50} (50% inhibitory concentration) was defined as the concentration of the compound that inhibited cell proliferation by 50%. These data are presented in Tables 2 and 3 In addition, in order to assess the possible mechanism of action, compounds **4i** and **5i** have also been evaluated against REH and K562 leukemia cells.

6.1.2. Trypan blue dye exclusion assay

The viability of the leukemic cells (REH, K562) was determined by Trypan blue dye exclusion assay [18] after treatment with **4i** and **5i**. Cells (0.5 × 10^5 cells/ml) were cultured for 24 h, following which increasing concentrations of the compounds (0–10 μM) were added and incubated. Cells treated with DMSO served as the vehicle control. Treated cells were collected after 48 and 72 h and viability was determined by trypan blue staining. Each experiment was repeated a minimum of three times and error bars were calculated and plotted.

6.1.3. MTT assay

To check the proliferation rate of the cells, following treatment with increasing concentrations of **4i** and **5i** (0–10 μM), REH and K562 cells (0.5 × 10^5 cells/ml) were harvested after 48 and 72 h and used for the MTT assay [19,20]. Cells treated with equal amount of DMSO served as vehicle control. Experiments were repeated three independent times, each in duplicate, and bar diagrams were plotted with error bars.

6.1.4. Live dead assay

4i mediated cell death in REH and 293T cells were studied using live dead assay. Ethidium bromide is excluded by live cells with intact membrane, but it can enter dead cells with broken membrane and stains the DNA. The cells were seeded (1 × 10^5/ml) in 6 well plates and **4i** (0.5 μM) was added to both Reh and 293T cells. DMSO served as vehicle control. Cells were harvested after 48 h, stained with ethidium bromide (5 μg/ml) and subjected to flow cytometry.

6.1.5. Cell cycle analysis

REH cells (0.5 × 10^5 cells/ml) were cultured for 24 h and compounds **4i** or **5i**, were added (0, 0.1, 0.5 and 1 μM) to the culture and incubated. Cells were harvested after 48 h, washed, fixed with 70% chilled ethanol and analyzed using flow cytometry following staining with propidium iodide, as described previously [20]. A minimum of 10,000 cells were acquired per sample and histograms were analyzed using WinMDI 2.8 software. Experiments were repeated two independent times and cell cycle phase was plotted in bar diagram with error bars.

6.1.6. Detection of intracellular ROS production by flow cytometre

The total intracellular ROS production was measured using cell permeable fluorescent probe 2,7-dichlorodihydro fluorescein diacetate (H_2DCFDA) in REH cells as described previously [21]. REH cells were treated with 1 μM of **4i** for different time points (5, 15, 30 and 60 min), cells were harvested, washed with 1× phosphate-buffered saline and incubated with 0.5 μM H_2DCFDA at 37° C for 15 min and fluorescence intensity was analyzed by flow cytometry (FACS Calibur, BD Biosciences, USA). Cells treated with H_2O_2 were served as the positive control.

6.1.7. DNA fragmentation assay

Fragmentation of genomic DNA due to apoptosis was detected by agarose gel electrophoresis [18]. Briefly, REH cells were treated with increasing concentrations (0, 0.1, 0.5, 1 and 5 μM) of **4i** for 48 h. DMSO treated cells were used as a vehicle control. Total genomic DNA was isolated using a standard protocol [22]. After 48 h treatment, cells were harvested and washed with 1X PBS, lysed in lysis buffer (100 mM NaCl, 10 mM Tris pH 8.0, 0.25%Triton X-100, 1 mM EDTA and 200 μg/ml Proteinase K), incubated at 55 °C for 5 h. RNase treatment was applied (50 μg/ml) for 1 h at 37 °C, samples were deproteinized using phenol:chloroform and DNA content was precipitated using 1/10th volume of 3 M sodium acetate (pH 5.2) and an equal volume of isopropanol. The pellets were washed with 70% ethanol, dried, dissolved in TE (10:1), loaded on 2% agarose gel and run at 50 V for 3 h.

6.1.8. Annexin V-FITC flow cytometric analysis

Phosphatidylserine exclusion on apoptotic cells was detected by Annexin V-FITC staining (Santa Cruz, USA). Briefly, REH cells were treated with **4i** (1 μM) and equivalent DMSO-treated control cells were harvested, washed with phosphate-buffered saline and resuspended in binding buffer (HEPES-10 mM pH 7.4, 144 mM NaCl and 25 mM $CaCl_2$), stained with Annexin V-FITC (0.2 mg/ml) and propidium iodide (0.05 mg/ml) for 20 min on ice and analyzed in a flow cytometer [18].

6.1.9. Measurement of mitochondrial membrane potential

Mitochondrial transmembrane potential after treatment with **4i** was measured using JC-1 (5, 5′, 6, 6′-tetrachloro-1, 1, 3, 3′-tetraethylbenzimidazolcarbocyanamide iodided; Calbiochem, USA) dye as described earlier [18]. Briefly, after 48 h of treatment with **4i** (0.5 and 1 μM), cells were harvested and incubated at 37 °C for 20 min with JC-1 (0.5 μM), washed and analyzed by flow cytometry. 2,4-DNP was used as a positive control. Typical green versus red ratio of JC-1 florescence was represented with bar diagrams with error bars using two independent experiments.

6.1.10. Statistical analysis

The values were expressed as mean ± SEM for control and experimental samples and statistical analysis was performed using One-way ANOVA followed by Dunnett test and significance was calculated after comparing each value with control, for the analysis, using GraphPad software prism 5.1. The values were considered as statistically significant, if the *p*-value was equal to or less than 0.05.

Acknowledgments

We gratefully acknowledge the support for this research effort from All India Council for Technical Education (AICTE), New Delhi (Ref. No. 8023/BOR/RID/RPS-169/2008-09) for SSK. The cytotoxic activities were determined by financial support of the KU Leuven (GOA 10/014). We thank Ms. Mrinal Srivastava. We would also like to thank NMR facility, Indian Institute of Science, Bangalore for characterisation of all compounds. We also thank FACS facility, IISc for flow cytometric studies. We thank Lizette van Berckelaer for the cytostatic determinations.

Appendix A. Supplementary data

Supplementary data related to this article can be found at http://dx.doi.org/10.1016/j.ejmech.2014.07.054.

References

[1] S.S. Karki, K. Panjamurthy, S. Kumar, M. Nambiar, S.A. Ramareddy, K.K. Chiruvella, S.C. Raghavan, Synthesis and biological evaluation of novel 2-aralkyl-5-substituted-6-(4′-fluorophenyl)-imidazo[2,1-*b*][1,3,4]thiadiazole derivatives as potent anticancer agents, Eur. J. Med. Chem. 46 (2011) 2109–2116.

[2] G. Kolavi, V. Hegde, I.A.M. Khazi, Intramolecular amidation: synthesis of novel imidazo[2,1-*b*][1,3,4]thiadiazole and imidazo[2,1-*b*][1,3]thiazole fused diazepinones, Tetrahedron Lett. 47 (2006) 2811–2814.

[3] A.K. Gadad, M.N. Noolvy, R.V. Karpoormath, Synthesis and anti-tubercular activity of a series of 2-sulfonamido/trifluoromethyl-6-substituted imidazo [2,1-*b*]-1,3,4-thiadiazole derivatives, Bioorg. Med. Chem. 12 (2004) 5651–5659.

[4] R.S. Lamani, N.S. Shetty, R.R. Kamble, I.A.M. Khazi, Synthesis and antimicrobial studies of novel methylene bridged benzisoxazolyl imidazo[2,1-*b*][1,3,4] thiadiazole derivatives, Eur. J. Med. Chem. 44 (2009) 2828–2833.

[5] S. Orrenius, B. Zhivotovsky, P. Nicotera, Regulation of cell death: the calcium-apoptosis link, Nat. Rev. Mol. Cell. Biol. 4 (2003) 552–565.

[6] G. Kroemer, J.C. Reed, Mitochondrial control of cell death, Nat. Med. 6 (2000) 513–519.

[7] A.H. Blatt, Organic Synthesis Coll, vol. 2, John Wiley & Sons, pp. 480.

[8] J. Hartung, M. Schwarz, Towards improved alkoxyl radical precursors – the synthesis of N-alkoxy-4-(*p*-chlorophenyl)thiazole-2(3H)-thiones, Synlett 7 (1997) 848–850.

[9] T. Ganesh, Ch Harish Kumar, G.L. David Krupadanam, A facile synthesis of 2-hydroxy-2-aryl-1,4-benzodioxanes, Synth. Commun. 29 (1999) 2069–2078.

[10] D.L.J. Clive, S. Hisaindee, D.M. Coltart, Derivatized amino acids relevant to native peptide synthesis by chemical ligation and acyl transfer, J. Org. Chem. 68 (2003) 9247–9254.

[11] M. Ogata, H. Matsumoto, S. Kida, S. Shimizu, K. Tawara, Y. Kawamura, Synthesis and antifungal activity of a series of novel 1,2-disubstituted propenones, J. Med. Chem. 30 (1987) 1497–1502.

[12] S. Ling, Z. Xin, Z. Qing, L. Jian-Bing, J. Zhong, F. Jian-Xin, Synthesis, structure and biological activity of novel 1H-1,2,4-triazol-1-yl-thiazole derivatives, Synth. Commun. 37 (2007) 199–207.

[13] S.A. Laufer, D.R.J. Hauser, A.J. Liedtke, Regiospecific and highly flexible synthesis of 1,4,5-trisubstituted 2-sulfanylimidazoles from structurally diverse ethanone precursors, Synthesis 2 (2008) 253–266.

[14] P. Wan, X. Xu, Disproportionation of 4-nitroacetophenone to 4-aminoacetophenone and 4-nitrobenzoic acid, J. Org. Chem. 54 (1989) 4473–4474.

[15] C.F. Koelsch, Bromination of 3-acetocoumarin, J. Am. Chem. Soc. 72 (1950) 2993–2995.

[16] S. Dhepe, S. Kumar, R. Vinayakumar, S.A. Ramareddy, S.S. Karki, Microwave-assisted synthesis and antimicrobial activity of some imidazo[2,1-*b*][1,3,4] thiadiazole derivatives, Med. Chem. Res. 21 (2012) 1550–1556.

[17] M. Srivastava, M. Nambiar, S. Sharma, S.S. Karki, G. Goldsmith, M. Hegde, S. Kumar, M. Pandey, R.K. Singh, P. Ray, R. Natarajan, M. Kelkar, A. De, B. Choudhary, S.C. Raghavan, An inhibitor of nonhomologous end-joining abrogates double-strand break repair and impedes cancer progression, Cell 151 (2012) 1474–1487.

[18] K.K. Chiruvella, V. Kari, B. Choudhary, M. Nambiar, R.G. Ghanta, et al., Methyl angolensate, a natural tetranortriterpenoid induces intrinsic apoptotic pathway in leukemic cells, FEBS Lett. 582 (2008) 4066–4076.

[19] C.V. Kavitha, M. Nambiar, C.S. Ananda Kumar, B. Choudhary, K. Muniyappa, K.S. Rangappa, S.C. Raghavan, Novel derivatives of spirohydantoin induce growth inhibition followed by apoptosis in leukemia cells, Biochem. Pharmacol. 77 (2009) 348–363.

[20] M.S. Shahabuddin, M. Nambiar, B. Choudhary, G.M. Advirao, S.C. Raghavan, A novel DNA intercalator, butylamino-pyrimido[4′,5′:4,5]selenolo(2,3-*b*) quinoline, induces cell cycle arrest and apoptosis in leukemic cells, Invest. New Drugs 28 (2010) 35–48.

[21] M. Hegde, S.S. Karki, E. Thomas, S. Kumar, K. Panjamurthy, Novel levamisole derivative induces extrinsic pathway of apoptosis in cancer cells and inhibits tumor progression in mice, PLoS One 7 (2012) e43632.

[22] M. Nambiar, S.C. Raghavan, Prevalence and analysis of t(14;18) and t(11;14) chromosomal translocations in healthy Indian population, Ann. Hematol. 89 (2010) 35–43.